Effect of salt water intrusion on the groundwater resources at Delta of wadi Kiraf area, Shaltein, Egypt

M. A. Abd Alla
National Research Institute of Astronomy and Geophysics[1]

A b s t r a c t : The hydrogeophyscial investigation plays a very important role in the assessment of groundwater in the Delta wadi Kiraf area. This area is located at the triangle Halaib-Shalatin area, Southeastern corner of Egypt. The present work was selected to show the drawbacks of the effects of saltwater intrusion on the groundwater potentiality using the vertical electrical sounding technique. Many conduit faults with different orientations are presented at or near to polluted sites.

Thirty vertical electrical sounding stations (VES) were conducted in the concerned area. The Schlumberger configuration was used with distances of current electrodes that varied from 1.5 m up to 600 m. The correlation of the deduced geoelectric parameters and the available geological information was helpful in establishing the specific resistivities of the formations.

The interpretation of the acquired resistivity field data led to the classification of the geoelectrical and geological successions to four geoelectric units; the first unit divided into two units corresponding to surface layer (first unit corresponding to wadi deposits and the second unit corresponding to high resistivity due to weathering materials), while the second unit is a sandstone layer saturated with fresh/brackish water, and the third geoelectrical unit has resistivity values less than one Ωm which reflects the existence of saltwater. The fourth geoelectrical unit: This layer represents the basement rocks (metamorphic rocks) and it appeared at VES's 41, 42, 43, 44 and 45. Its true resistivity values range between 25.2 and 5500 Ωm. It represents dry to saturated fractured basement rocks. Generally, resistivity values decrease with depth with the highest values of the unsaturated zone near the surface to the lowest values of saltwater saturated zone. The resultant models from resistivity measurements agree with other lithologic data. Also, The Least Squares ABIC technique was applied to the same data set. The results of the inversion process elucidate the lateral and vertical variations in lithology.

Key words: Wadi Kiraf, salt water intrusion, the least squares ABIC, groundwater

[1] Helwan, 11722 Cairo, Egypt; e-mail: tarakhan66@hotmail.com

1. Introduction

The study area is located at Delta wadi Kiraf in the southeastern corner of Egypt (Fig. 1). The present study is concerned with investigating the groundwater potentiality at the downstream of wadi Kiraf area. This area possesses a good quality-land that could be relined and cultivated. The major problem facing the construction of new communities or development of arid or semiarid regions is the source of water. The main problem of this area is that it is polluted by saltwater intrusion. The question is: to what extent does this phenomenon spread. The study area is situated in the coastal plain covered with marine sediments and the Precambrian dissecting it. Groundwater occurs under various geological conditions including joints, fractured highly weathered basement rocks. The hydrographic parameter was calculated for each basin manually *(Mina et al., 1996)*. Surface resistivity surveys have been used successfully to determine the aquifer; locate fresh, brackish, and saline water zones *(Van Overmeeren, 1989)*.

Thirty vertical electrical soundings (VES) were measured in the field by

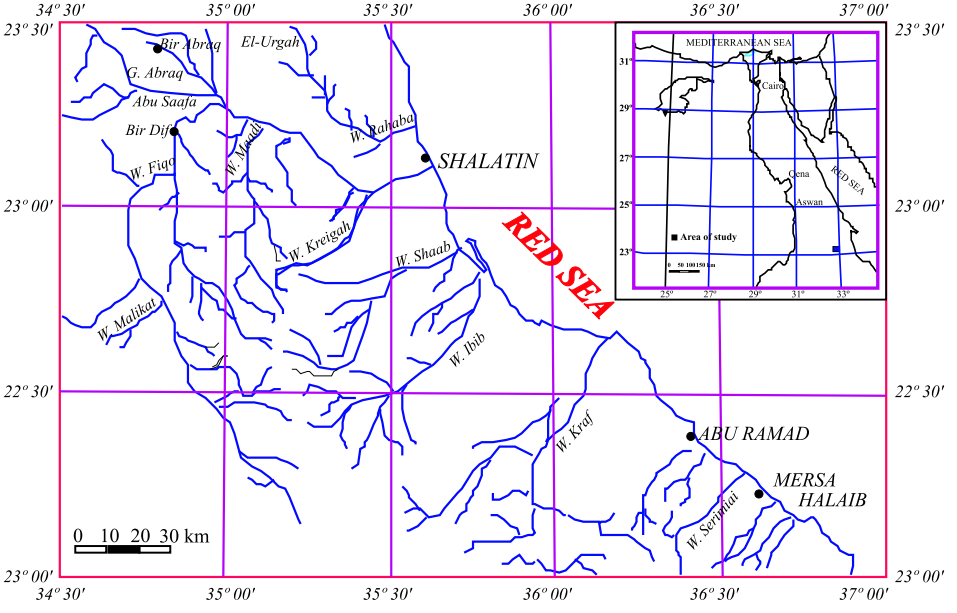

Fig. 1. Location map of the studied area.

using Schlumberger configuration and electrode spacing starting from 1.5 m up to 600 m. The quantitative interpretation of 1D geoelectrical measurements was discussed by several authors; among them *Koefoed (1965, 1979); Kunetz and Rocroi (1970); Gosh (1971)* and *Zohdy (1975, 1989).* The measured resistivity soundings were processed by using *IPI software (2000).* Also, a 2D inversion technique based on the ABIC least squares method was carried out on the acquired data.

2. Geomorphological and geological setting

Wadi Kiraf comprises one hydrographic basin. This wadi is surrounded by mountains. The wadi drains its seasonal surface water to Red Sea. The hydrographic parameters were calculated by *Mina et al. (1996).*

There are two rock units which predominantly in Halayiab and Shalaten area (about 300 km^2), metamorphic and magnetic, both of late Precambrian age, unconformably overlained by Mesozoic sandstone and Tertiary (Red Sea) marine sediments *(Mina et al., 1996).*

Lithologic units were recognized as follow *(Nasr et al., 1994)*:

Quaternary: Wadi alluvium1 units are represented by wadi Sabkha, deposits and undifferentiated Quaternary deposits.

Tertiary: Basalt, alkali granite, lava and agglomerates.

Cretaceous: It is represented by Abu-Aggag Formation Sandstone (Nubian group).

Late proterozoic: Magnetic rocks, metamorphic rocks.

Structural analysis: The area is affected by numerous faults (Fig. 2) the area can be divided into four sets *(Mina et al., 1996)* as follows: NE-SW, E-W, N-S, NW-SE.

3. Hydrogeological setting

As it is obvious from the geologic setting in the study area, formation of the Upper Cretaceous overlies the basement rocks. Consequently, it is the only probable water-bearing formation in this area. It is worthy to mention that Tertiary volcanic rocks are exposed along faults bounding the

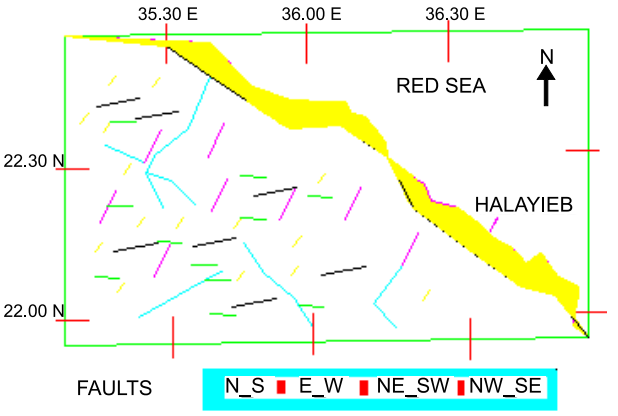

Fig. 2. Lineaments of Halayieb area.

main stream of wadi Kiraf. This situation leads to the continuous existence of salt water intrusions that spread from several kilometers towards the western direction *(Fathy et al., 2003)*.

4. Geophysical survey and data processing

The main targets of the present study are to delineate the geometry of the aquifer, and also to determine the subsurface geological and hydrological conditions by using the Schlumberger configuration of the vertical electrical sounding technique. The objectives of using the VES are to deduce the variation of resistivity with depth and to correlate it with the available geological information from the boreholes located in the study area.

Thirty VES stations were measured (Fig. 3) using electrode spacing starting from AB/2 = 1.5 up to 600 m, in successive steps according to the topography and perpendicular to the coastal plain. Sounding data are interpreted using *IPI2WIN software (2000)* to compute the true depths and resistivities for each VES curve. The results of interpretation of the measured field sounding data revealed the existence of four geoelectric units.

The plotted curves in the study area may be classified into three groups; A, B and C. The characteristic curves of each group are shown in (Fig. 4). Type A curves reflect bedrock of high resistivity by sleepily rising apparent

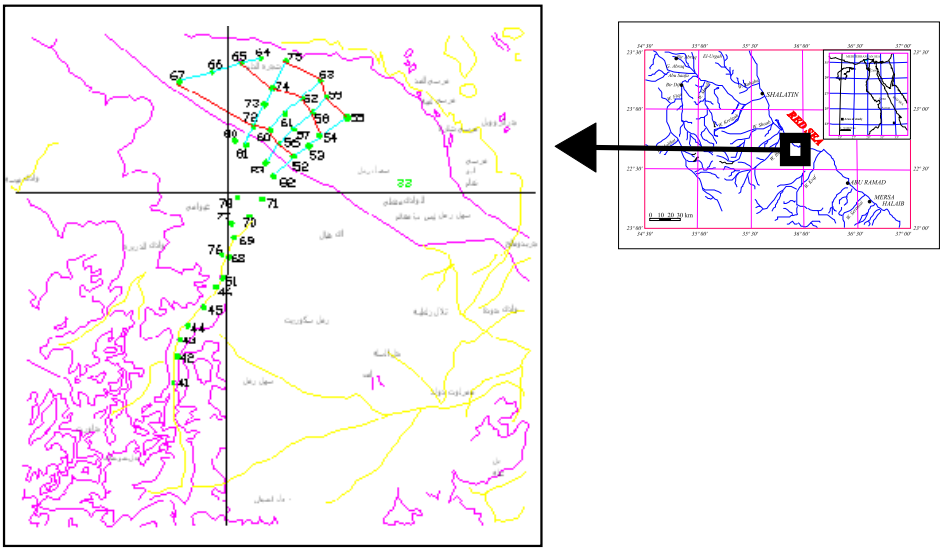

Fig. 3. Location map of VES sounding.

resistivities at large electrode spacing. The most common types of curves in the area are B and C. These curves decline to very low resistivity values (apparent resistivity $\rho_a < 10\,\Omega$m) at large electrode spacing.

Therefore, some results of 1D inversion are not fully satisfying for actual 3D geologic structure. We present a 2D inversion for the same data set using *Uchida's (1991)* algorithm to get a comprehensible solution. The algorithm is based on the ABIC technique (Akaike Bayesian Information Criterion, *Akaike, 1980*) and applies the optimum smoothness using a finite element calculation mesh, to obtain the convergence.

The algorithm considers a 2-D-earth model, whose resistivity varies along the x and z axes, while it does not change along the y axis. As much the current is injected at a point on the surface, however, it flows three dimensionally in the Earth; the response in a 2-D Earth is given by Poisson's equation as

$$-\nabla[\sigma(x,z)\nabla V(x,y,z)] = I(x,y,z), \tag{1}$$

where $\sigma(x,z)$ is the conductivity, $V(x,y,z)$ is the electric potential, and $I(x,y,z)$ represents the source current intensity. By applying the Fourier

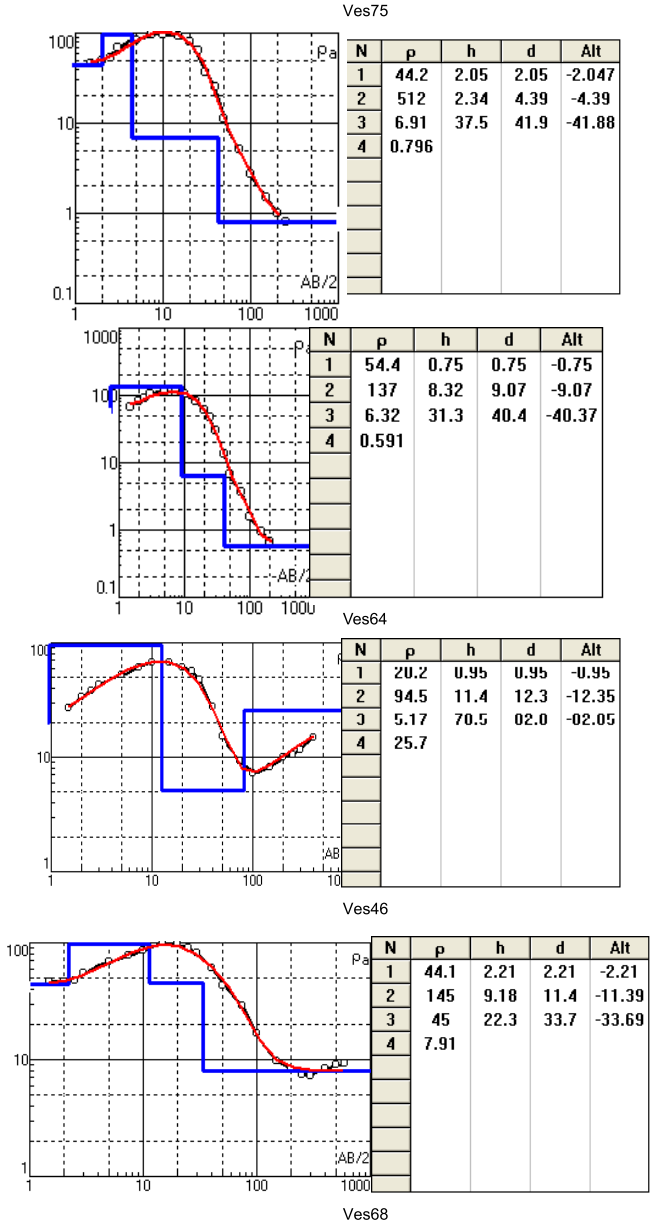

Fig. 4. Example of interpretation curves by IPI program.

transform to Eq. (1) with respect to the y coordinate, we obtain

$$-\nabla[\sigma(x,z)\nabla\hat{V}(x,k_y,z)] + k_y^2\sigma(x,z)\hat{V}(x,k_y,z) = \hat{I}(x,k_y,z), \tag{2}$$

where $\hat{}$ is the Fourier transform, and k_y is the Fourier transform variable. Then, applying the inverse Fourier transform

$$\Delta V(x,0,z) = (1/\pi)\int_0^\infty \hat{V}(x,k_y,z)dk_y, \tag{3}$$

the apparent resistivity for Schlumberger can be calculated as

$$\rho_a = \frac{G\Delta V}{I}, \tag{4}$$

where G is a geometrical factor that depends on the electrode arrangement and their spacing, and ΔV is the calculated potential difference between the receiving electrodes M and N. A detailed explanation of the finite-element discretization of Eq. (2) is given in *Sasaki (1981)*. Further details about the algorithm and convergence criteria can be found in *El-Qady et al. (1999)*.

The ABIC has been proposed by applying the maximum entropy theorem to the Bayesian statistical. ABIC is derived to provide an index for finding the maximum Bayesian likelihood as:

$$ABIC = 2\log(\max.L(m/d)) + 2\dim\ (\text{hyperparameter}), \tag{5}$$

Where $L(m/d)$ is the Bayesian likelihood and the hyperparameter means a parameter, which is not used to express the model directly, but used to obtain parameters of the model. The only hyperparameter in this case is the smoothing parameter (α). Further explanation of the equations was described by *Uchida (1993)*, then ABIC can be written

$$ABIC(\alpha) = N\log\left(2\pi\frac{U}{N}\right) - \log\left|\alpha^2C^TC\right| + \log\left|(WA)^T(WA)\right| + \\ + \alpha^2C^TC + N + 2, \tag{6}$$

where d is a set of observed data, A is a Jacobian matrix defined by $A_{ij} = \partial y_i/\partial\rho_j$, m is a hypothetical model, W is a diagonal weighting, C is a roughness matrix of a model parameter, which gives the finite difference of the model parameters between laterally and vertically adjacent blocks and U is a function defined as:

$$U = \text{misfit} + \text{roughness penality of the model} = \phi + \alpha^2 \|Cm\|^2, \quad (7)$$

5. One-dimensional interpretation

Quantitative interpretation technique was applied to determine the thicknesses and true resistivities of the successive layers below each VES station using the measured field curves. The interpretation of the obtained VES curves is carried out using the software prepared by *Zohdy (1989)* and *Van der Velpen (1988)*. Then the results models are used as initial models for *IPI2WIN software (2000)* to compute the true depths and resistivities for each VES curve. The results of interpretation of these vertical electrical soundings revealed the existence of four major geoelectric units.

The main geoelectric units of the 1-D inversion have been collected to form geoelectrical cross-sections along five profiles portraying the subsurface setting in the study area. Only three geoelectric cross-sections are displayed in Figs. 5, 6 and 7. The interpretation of the geoelectric cross-sections indicates that the shallow subsurface lithological sequence in the study area is made up of four geoelectric zones of relative resistivities $\rho_1 > \rho_2 > \rho_3$.

1. The first geoelectrical unit: It represents wadi deposits. The true resistivity values are ranging from 8.16 to 3789 Ωm. It consists of more than one layer at some locations. It is composed mainly of dry sands mixed with other weathering materials.
2. The second geoelectrical unit: This layer represents the top part Cretaceous Sandstone (Nubian group). Its true resistivity values varied from 2.4 Ωm to 31 Ωm, with a maximum thickness of 28 m at VES 26. It corresponds to sandstone layer, which is considered as the main groundwater aquifer in the study area and contains fresh and brackish water.
3. The third geoelecrical unit: This layer is rather thick and is totally saturated by salt waters as revealed from its ρ_t values, which range between 0.6 and 1.7 Ωm.
4. The fourth geoelectrical unit: This layer represents the basement rocks (metamorphic rocks) and it appeared at VES's 41, 42, 43, 44 and 45. Its true resistivity values range between 25.2 and 5500 Ωm. It represents

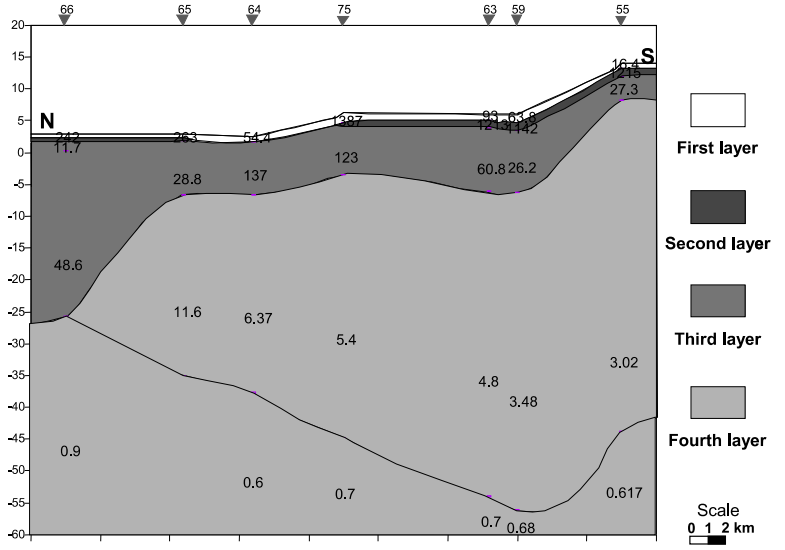

Fig. 5. Cross-section one dimension P1–P1′.

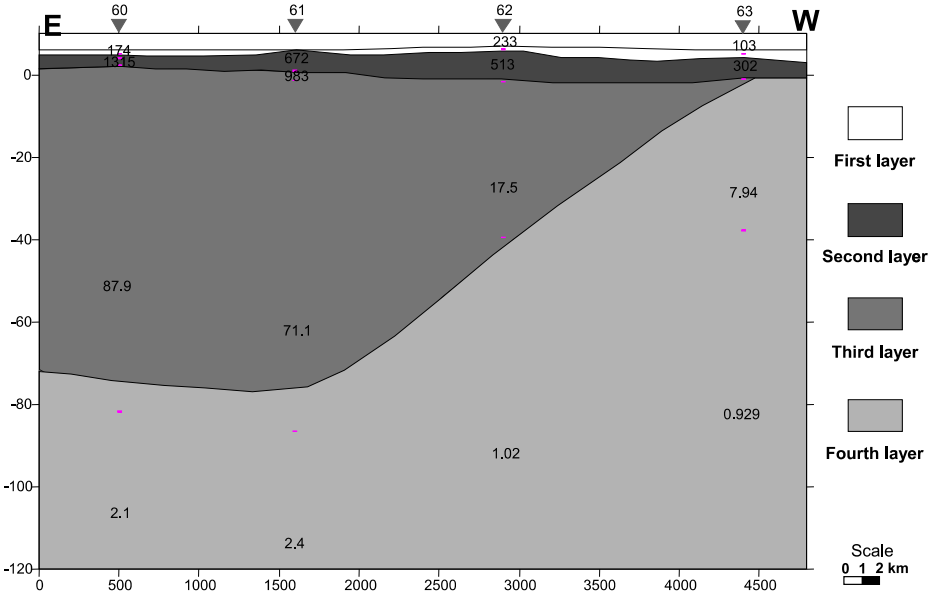

Fig. 6. Cross-section one dimensional P3–P3′.

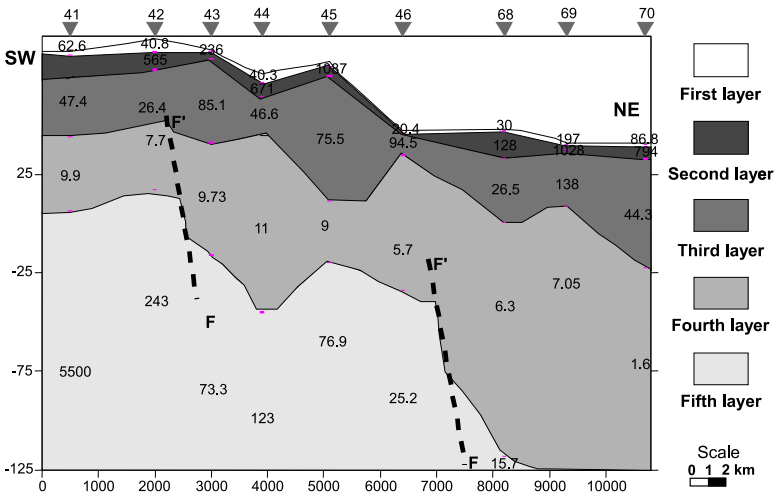

Fig. 7. Cross-section one dimensional P6–P6′.

dry to saturated fractured basement rocks. These volcanics are exposed nearby the investigated sites. They are associated with conduit faults.

6. 2D inversion results

During the inversion process, the program seeks a model that minimizes both the data misfit and the model roughness. From a statistical point of view, ABIC works as an index to determine the maximum likelihood of the model. That means, a smaller ABIC, indicates a larger likelihood and higher entropy, hence gives a best-fit model. This also means that the optimum smoothness is judged by minimizing ABIC, which makes the convergence and the selection of the optimum smoothness is objective. So, we have to run the inversion process until the best fit is attained.

Fig. 8 shows the RMS misfit and the smoothing factor (α) as a function of iteration number. As it is obvious in Figs. (8-a, 8-c and 8-f), line 1, line 3 and line 6 both RMS and α attains minima at the sixth iteration. This indicates that the sixth iteration's model is the best-fit model for these profiles 1, 3 and 6. For the profiles 2 and 4 (Figs. 8-b and d), the RMS

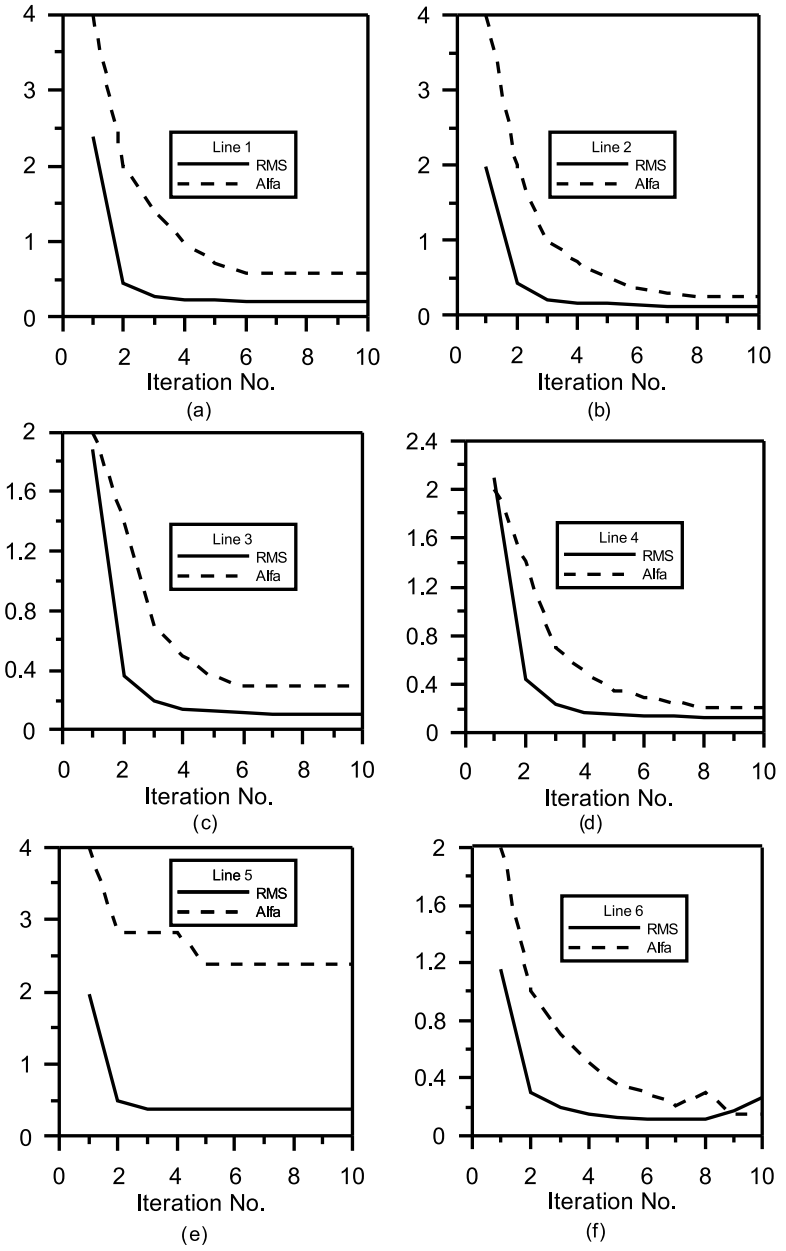

Fig. 8. RMS error and smoothing factor, as a function of iteration number during the 2-D inversion for some profiles.

and smoothing factor (α) attain the minima at the eighth iteration. As for profile 5 (Fig. 8-e) they attain it at the fifth iteration for the profile 5.

Fig. 9 shows a good correlation between the measured observed data and the response of the inverted model at some selected stations.

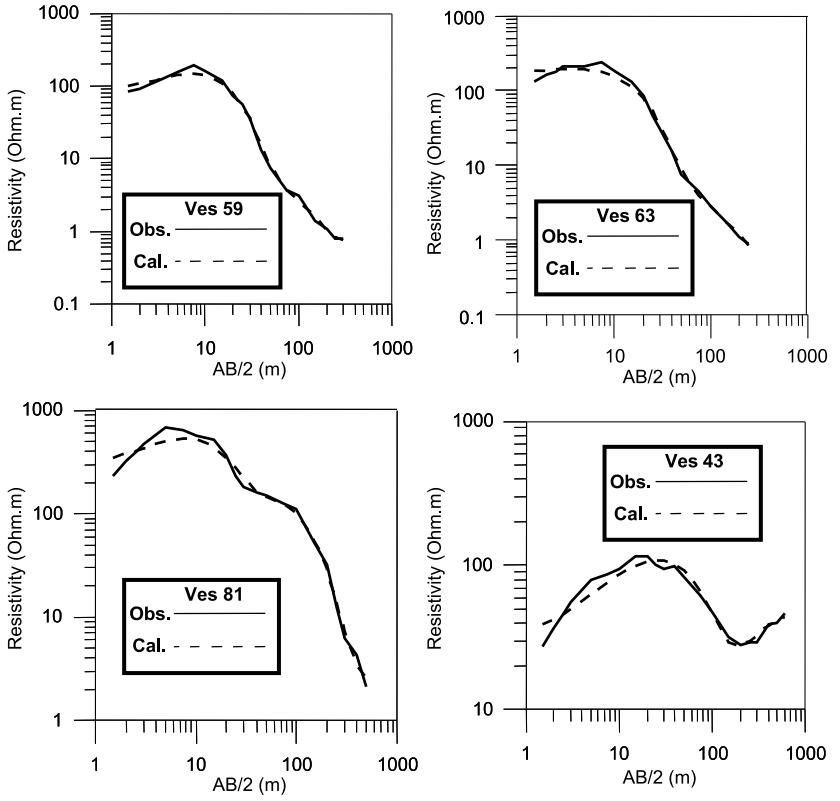

Fig. 9. Correlation between observed and calculated data for some VESes.

7. 2D cross-section

According to the results obtained through the inversion process, we could be able to construct the 2D-geoelectrical cross-section for each profile. This depending up on which iteration minimizes ABIC and gets the convergence.

The inverted 2-D cross-section for profile 1, which results from the sixth iteration, is displayed in (Fig. 10); as example it represents the profiles P1, P2, P3 and P5. The initial model is assumed to be a 100 Ωm homogeneous earth and the topography is incorporated in the modeling. We used 127 resistivity blocks in the inversion. Inspection of cross-sections P1–P1′ (Fig. 10) reveals a number of geoelectric layers of variable resistivities. The first geoeletric layer at the top of the profile acquires relatively medium to high values of resistivity, which correspond to surface layer (wadi deposits). The second geoelectrical units is also of high resistive values, which corresponds to fractured basement rocks. The third geoelectrical units may describe the saturated sand (fresh water aquifer). The fourth geoelectrical unit has very low resistivity values due to the effect of salt water intrusion. This kind of pollution is attributed to the presence of Tertiary volcanics. These volcanics are exposed nearby the investigated sites. They are associated with conduit faults, which are responsible for this pollution. Its ρ_t values range between 0.6 to 11.6 Ωm.

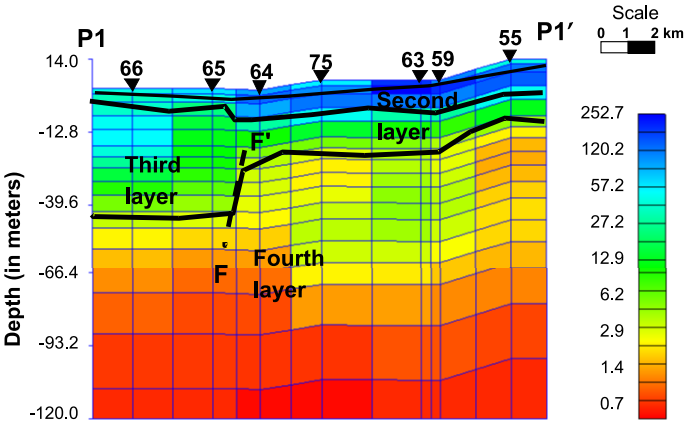

Fig. 10. 2D cross-section P1–P1′.

Fig. 11 shows the 2D cross-section of the inverted model after the sixth iteration for the profile P6. The initial model is assumed to be a 100 Ωm homogeneous earth and the topography is incorporated in the modeling. The number of the observed data used for the inversion is 194, while the number of resistivity blocks is 150 block. The general feature of this in-

verted section is as follows: The uppermost layer is the thin layers (wadi deposits), underlain by the second high resistive layer, which correspond to fractured basement. Below this layer, there is medium to course sand. This layer maybe forms the fresh water aquifer. The fourth layer is rather thick and is totally saturated by salt waters intrusion. The last geoelectric layer is composed mainly of sand and fracture basement rocks with resistivity ranging between 15.7 and 5500 Ωm. This layer maybe also saturated with salt water intrusion. This layer is dissected by normal faults.

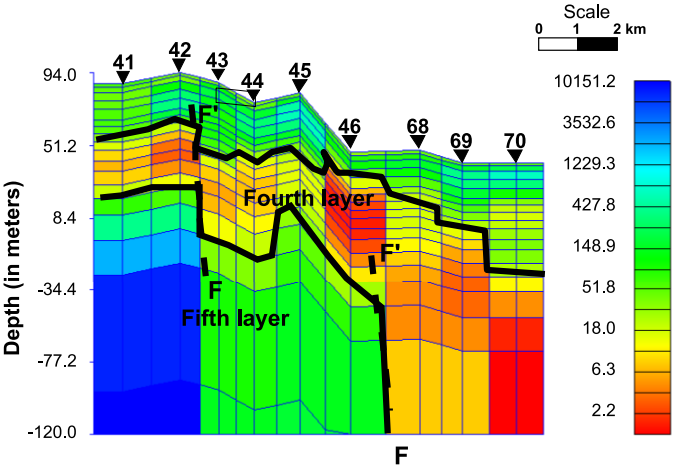

Fig. 11. 2D cross-section P6–P6′.

8. Conclusions

Due to the high demand for new agricultural area outside the Nile Valley. The Egyptian Government decided to develop Halaib-Shalatin area. The Government wanted to drill a new water supply in Delta wadi Kiraf area. Salt water intrusion was a possible problem.

We preformed a geophysical investigation using Vertical electrical sounding. This method is chosen for their low cost and usefulness in defining the expected targets. Salt water is very electrically conductive and is easily detected with electrical techniques. Electrical resistivity technique was used to determine whether the groundwater was brackish or fresh. The present

area of study is subject to enormous system of faults. These faults caused the groundwater to be polluted by salt water intrusion.

Thirtynine Schlumberger VES stations were interpreted in 1D and 2D ABIC least squares. According to the results obtained, it can be concluded that the inversion procedure can reduce the misfit through the iteration. The 2D resultant cross-section had been correlated with the 1D inversion. There is good agreement between them especially in P1–P1′ and P3–P3′, but in cross-section P6–P6′. The results show that the studied section is classified into four geoelectrical layers. The fourth geoelectrical unit has very low resistivity values due to the effect of salt water intrusion. This kind of pollution is attributed to the presence of Tertiary volcanics.

Acknowledgments. The author would like to thank Dr. Rafik G. Fathy (GARPAD) for providing the data of this work. The author expresses his indebtedness to Dr. Gad El-Qady for running the 2-D resistivity inversion code, his efforts to enhance the manuscript to its present form. I would like to express my gratitude to the stuff members of the geoelectrical laboratory NRIAG.

References

Akaike H., 1980: Likelihood and Bayes procedure. In: Bayesian statistics, J. M. Bernardo, et. al. (ED)., Univ. press, Valencia, Spain. 143–166.

El-Qady G., 1999: 2D inversion of VES data in Saqqara archaeological area, Egypt. Earth Planets. Space, 51, 1091–1098.

Fathy R. G., AbdAll Mohamed A., Nagaty M. El-amir, Atya M. A., 2003: Contribution to the effect of salt water intrusion on the groundwater resources at Delta Wadi Hodein, Shalatein Area, Southeastern Desert, Egypt. Journ. Appl. Geophys., **2**, 199–210.

Gosh D. P., 1971: The application of linear filter theory to the direct interpretation to geoelectrical sounding measurements. Geophys. Prosp., **19**, 192–217.

Koefoed O., 1965: Direct methods of interpretating resistivity observations. Geophys. Prosp., 13.

Koefoed O., 1979: Geosounding principlles-1, Resisitivity sounding measurements, methods in geochemistry and geophysics. Elsevier Pub.

Kunetz G., Rocroi J., 1970: Traitment automatique des sondoges electrique. Geophys. Prosp., **18**, 157–198.

Mina M., Shatya F., Mansour S., Hassan A., 1996: Exploration for groundwater at the area between Halayieb and Shalaten, Eastern Desert, Egypt. Proc. Geol. Surv. Egypt Cenn. Conf., 581–598.

IPI2Win-1D Program, 2000: Programs set for 1-D VES data interpretation. Dept. of Geophysics, Geological Faculty, Moscow University, Russia.

Nasr B. B., Beniamin N. Y., Tolba M. I., Yossef M. M., El-Sherbini H., Makhlof A. A., 1994: Geology of Gabal Elba Area South Eastern Desert of Egypt. Internal Report, Geological Survey of Egypt.

Sasaki Y., 1981: Automatic interpretation of resistivity sounding data over two-dimensional structures (I). Geophys. Explor. of Japan (Butsuri Tanko), **34**, 341–350 (in Japanese).

Uchida T., 1991: 2 D resistivity inversion for Schlumberger sounding. Butsuri-Tansa, **44**, 1, 1–17.

Uchida T., 1993: Smooth 2-D inversion for Magetotelluric Data Based on Statistical Criterion ABIC. J. Geomag. Geoelectr., V., 45, 841–858.

Van der Velpen D. B. A., 1988: Resist, a computer program for the interpretation of resistivity sounding curves. An ITC. M. Sc. Research Project. ITCD, Delft, The Netherlands.

Van Overmeeren R. A., 1989: Aquifer boundaries explored by geoelectrical Measurements in the coastal plain of Uemen: A case of equivalence.

Zohdy A. R., 1989: A new method for automatic interpretation of Schlumberger and Wenner curves. Geoph., **54**, (2), 245–253.

Zohdy A. A. R., Eaton G. P., Mabey D. R. 1975: Automatic interpretation of Schlumberger sounding curve using Dar Zarrouk functions, U. S. Geol. Surv., Bull., 313-e, 39 p.